Chemosensors for Lead(II) and Alkali Metal Ions Based on Self-Assembling Fluorescence Enhancement (SAFE)

Wen-Sheng Xia,[†,§] Russell H. Schmehl,[*,†] Chao-Jun Li,[*,†] Joel T. Mague,[†] Chu-Ping Luo,[‡] and Dirk M. Guldi[‡]

Department of Chemistry, Tulane University, New Orleans, Louisiana 70118, and Radiation Laboratory, University of Notre Dame, Notre Dame, Indiana 46545

Received: August 24, 2001

A class of bis-crown ether fluorescent chemosensors for detection of trace amounts of Na^+, K^+, and Cs^+ and Pb^{2+} was investigated. A distyrylbenzene derivative with crown ether rings of varying size attached to each benzene (12-crown-4 (**1**), 15-crown-5 (**2**), and 18-crown-6 (**3**)) can form intermolecular sandwich structures with Na^+, K^+, and Cs^+ ions, respectively. In addition, bis-crown **2** forms unique sandwich complexes with Pb^{2+}; the stoichiometry depends on the counterion present. Crystal structure data for the complex of $Pb(CF_3COO)_2$ with **2** indicate a unique sandwich structure having dilead tetrakis(trifluoroacetate) bridging two crowns on separate ligands. The bis-crown/alkali metal ion complexes have 1:1 stoichiometry in each case. ^1H NMR spectra and MALDI-TOF mass spectra clearly demonstrate that formation of the self-assembled sandwich structure is associated with the fluorescence enhancement for sensor molecules **2** and **3** with K^+ and Cs^+, respectively. Sensor molecule **1**, however, has an additional fluorescence enhancement mechanism, which involves contributions from the formation of excimers.

Introduction

While there has been rapid development of modern analytical techniques for application in clinical and environmental science, there is still a significant need to provide real-time monitoring methods for the detection of trace amounts of specific analytes in solution.[1] Although currently available methods (i.e. potentiometric) are quite sophisticated, the techniques often have complicated preparations and significant lag times for analysis.[2] Optical sensors, particularly those involving fluorescence, are growing in importance among methods for in situ analysis of trace analytes.[3] Fluorescence-based chemosensors have received considerable attention in recent years since fluorescence measurements can be readily obtained from the chemosensor in solution or at interfaces, often at very low concentrations of analyte.[4]

One effective group of fluorescent chemosensors for alkali metal, alkaline earth metal, and select heavy metal ions involves chromophores having covalently linked crown ether substituents. Crown ether derivatives are known to form complexes with various cations and anions selectively.[5] These chemosensors show significant cation-induced changes in absorption or fluorescence spectra.[6] Fluorescence sensing often involves changes in luminescence via PET (photoinduced electron transfer),[7] charge transfer,[8] and excimer formation[9] after the crown coordinates the analyte. Recently, Finney and co-workers illustrated that fluorescent enhancement could also be observed upon rigidification of a chromophore following substrate binding.[10] A number of these systems have been used as optical sensors and as functional units of ionic photoswitchable devices.[11]

Among the alkali metal ions, Na^+, K^+, and Cs^+ have attracted particular interest because the first two ions are ubiquitous in nature and are especially important in clinical analysis and $^{137}Cs^+$ appears in nuclear reactor waste. Currently there is no available fluorescent chemosensor that can detect K^+ and avoid interference from the large excess of Na^+ ($Na^+/K^+ \approx 30$) typically present under physiological conditions.[1,3] Recently, Masilamani et al.[3] reported that a cryptand-based fluorescent molecular sensor shows moderate selectivity toward K^+ over Na^+. However, a potassium-selective fluorescent molecular chemosensor with a practical selectivity over sodium is yet to be developed.

The detection of cesium has only recently received attention because of potential leakage of ^{137}Cs from nuclear waste storage facilities.[12] Currently, there is no effective method available to detect small amounts of Cs^+ from nuclear waste solutions. Very recently, Dabestani et al.[13] developed a first-generation Cs^+-selective fluorescence chemosensor based on a calix[4]arene derivative. This elegant chemosensor, while sensitive to the presence of Cs^+, also binds other alkali metal ions with reasonably high affinity. As a result, there is a need to develop other Cs^+ chemosensors that have higher selectivity.

There has also been interest in the development of Pb^{2+} chemosensors employing fluorescence detection. Chen and Sullivan developed a Re(I) complex having a pendant aza-crown that selectively binds Pb^{2+} and exhibits a significant luminescence intensity increase via inhibition of intramolecular photoinduced electron transfer.[14] Very recently, Godwin and coworkers[15] developed a new kind of ratiometric fluorescent sensor for Pb^{2+} consisting of a fluorescent dansyl with an amino terminus of a tetrapeptide. This system showed good selectivity to Pb^{2+} ions in solution.

It is known that various crown ether derivatives can form sandwich complexes with particular alkali metal ions and Pb^{2+}.[5] For instance, while benzo-15-crown-5 forms complexes with Li^+, Na^+, and K^+, a sandwich complex is only formed with K^+.[16] Similarly, benzo-18-crown-6/Cs^+ and benzo-12-crown-4/Na^+ also form unique sandwich complexes. It is possible to

* Corresponding authors. E-mail: R.H.S., russ@tulane.edu; C.-J.L., cjli@tulane.edu.
† Tulane University.
‡ University of Notre Dame.
§ Currently at QTL Biosystems, Santa Fe, NM.

10.1021/jp013274x CCC: $22.00
Published on Web 01/03/2002

SCHEME 1

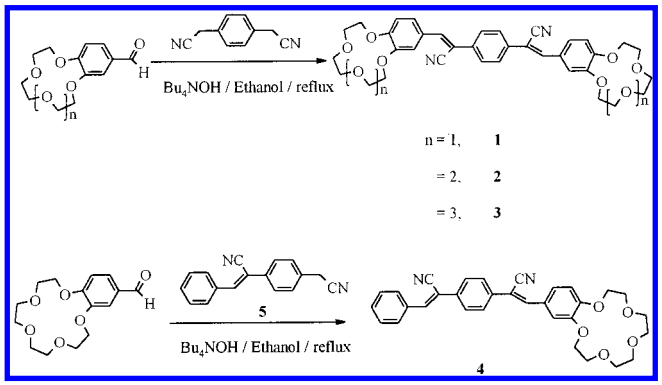

exploit this highly specific sandwich formation in the development of fluorescent chemosensors. By the coupling of particular benzo-crowns to chromophores that become fluorescent only upon sandwich complex formation, ion-specific chemosensors can be developed. In recent work we illustrated this approach using distyrylbenzene derivatives modified with benzo-crown ethers on each peripheral benzene (Scheme 1) as chemosensors; 15-crown-5 derivatives exhibit fluorescence enhancement selectively in the presence of K^+, and 18-crown-6 derivatives respond to Cs^+ selectively.[17]

Sensitive and selective fluorescence enhancement is observed upon the addition of Na^+ to **1**, K^+ to **2**, and Cs^+ to **3**. This work shows that the high selectivity and sensitivity of these chemosensors arises from what we have referred to as self-assembling fluorescence enhancement (SAFE), resulting from formation of sandwich structures upon complexation with particular alkali metal ions. Luminescence spectral studies with ligands **2** and **3**, along with analogues having a single crown ether attached to each chromophore, suggest that molecular "rigidification" is responsible for the observed fluorescence enhancement for K^+ and Cs^+ chemosensors. In addition, we report luminescence enhancement of ligand **2** in the presence of Pb^{2+}. Crystallographic results illustrate that bimetallic lead trifluoroacetate units form bridges between crowns on adjacent ligands. This article provides a more detailed analysis of alkali metal ion binding to ligands **1**−**3** and describes the binding of Pb^{2+} to **2**. In addition, the first direct structural evidence is presented to link the formation of sandwich complexes with observed luminescence enhancements in a bis-crown/chromophore system.

Experimental Section

1. Synthesis. The synthetic route for the chemosensors is shown in Scheme 1. Molecules **1**−**3** were synthesized by the following procedure using molecule **1** as an example.

A mixture of 4′-formylbenzo-12-crown-4 (100 mg, 0.4 mmol) and 1,4-phenyldiacetonitrile (30 mg, 0.2 mmol) with 3 drops of tetrabutylammonium hydroxide (40% water solution) in ethanol was refluxed for about 2 h and was filtered hot. After cooling, the yellow solid was then washed with methanol several times and then recrystallized from chloroform/methanol (2/8) twice to give a bright yellow solid of **1** (120 mg, yield 70%). ^{1}H NMR ($CDCl_3$, 400 MHz, δ ppm): 7.68 (s, 3H), 7.49 (s, 1H), 7.46 (dd, J = 2 Hz, 8 Hz, 1H), 7.00 (d, J = 8 Hz, 1H), 4.2 (m, 4H), 3.83 (m, 4H), 3.79 (m, 4H). ^{13}C NMR ($CDCl_3$, 100 MHz, δ ppm): 153.6, 150.9, 142.5, 128.3, 126.7, 119.4, 18.5, 117.6, 108.9, 72.8, 71.8, 71.6, 71.5, 70.2. Anal. Calcd for $C_{36}H_{36}N_2O_8$: C, 69.23; H, 5.77; N, 4.48. Found: C, 69.53; H, 5.58; N, 4.36. IR (KBr, cm^{-1}): 2926, 2865, 2205, 1505, 1276, 1138.

Molecule 2. ^{1}H NMR ($CDCl_3$, 400 MHz, δ ppm): 7.66 (s, 2H), 7.62 (d, J = 2 Hz, 1H), 7.48 (s, 2H), 7.35 (dd, J = 2 Hz, 8 Hz, 1H), 6.87 (d, J = 8 Hz, 2H), 4.15 (m, 4H), 3.87 (m, 4H), 3.70 (m, 8H). ^{13}C NMR ($CDCl_3$, 400 MHz, ppm): 151.6, 149.0, 142.4, 135.0, 126.7, 126.2, 125.1, 118.4, 113.1, 112.8, 107.5, 71.2, 70.4, 69.3, 68.6. Anal. Calcd for $C_{40}H_{46}N_2O_{10}$: C, 67.42; H, 6.18; N, 3.93. Found: C, 67.38; H, 6.15; N, 3.77. IR (KBr, cm^{-1}): 2927, 2871, 2210, 1518, 1276, 1141.

Molecule 3. ^{1}H NMR ($CDCl_3$, 400 MHz, δ ppm): 7.67 (s, 2H), 7.63 (d, J = 2 Hz, 1H), 7.48 (s, 1H), 7.34 (dd, J = 2 Hz, 8 Hz, 1H), 6.87 (d, J = 8 Hz, 1H), 4.27 (m, 4H), 3.97 (m, 4H), 3.83−3.67 (m, 12H). In some batches, the protons at 7.76 and 7.73 ppm may merge to be one single peak. ^{13}C NMR ($CDCl_3$, 100 MHz, δ ppm): 151.9, 149.8, 135.5, 127.7, 126.6, 125.3, 118.7, 113.8, 113.5, 108.1, 71.4, 71.2, 71.1, 69.9, 69.8, 69.6, 69.4. Anal. Calcd for $C_{44}H_{52}N_2O_{12}$: C, 66.00; H, 6.50; N, 3.50. Found: C, 65.46; H, 6.56; N, 3.39. IR (KBr, cm^{-1}): 2919, 2863, 2211, 1516, 1271, 1138.

Molecule **4** was synthesized by a similar path. Compound **5** (40 mg, 0.16 mmol) and 4′-formyl-benzo-15-crown-5 (50 mg, 0.16 mmol) were dissolved in methanol containing 2 drops of tetrabutylammonium hydroxide. The solution was refluxed for 1 h and filtered hot. The greenish solid obtained was then separated by preparative TLC using chloroform/methanol (10/0.5) as eluent twice. Due to the reversible reaction, most of the product is molecule **2**. A small amount of compounds contains *Z*−*E* (*trans*−*cis*) isomers. Finally, about 5 mg of pure molecule **4** was obtained as pale yellow solid. ^{1}H NMR ($CDCl_3$, 400 MHz, δ ppm): 7.9 (t, 2H), 7.72 (m, 4H), 7.60 (s, 1H), 7.49 (m, 4H), 7.37 (dd, J = 2 Hz, 8 Hz, 1H), 7.25 (s, 1H), 7.21 (m, 4H), 3.95 (m, 4H), 3.78 (m, 8H).

Synthesis and Crystal Structure of 2−Pb(CF$_3$COO)$_2$ (C$_{50}$H$_{47}$F$_{12}$N$_3$O$_{18}$Pb$_2$). Crystals were obtained by the following method. To 10 mg of **2** suspended in 5 mL of acetonitrile solution was added 1 equiv of $Pb(CF_3COO)_2$ dissolved in CH_3CN. The solution was warmed until clear, filtered, and allowed to cool to room temperature where it was stored for 4−7 days. Yellow crystals were obtained and washed with CH_2Cl_2 and CH_3CN in situ to avoid drying. M_r = 1620.29. Crystal data: 0.30 × 0.43 × 0.53 mm; triclinic, space group $P\bar{1}$ (No. 2); a = 11.516(1), b = 12.133(1), c = 12.559(1) Å; α = 101.209(9), β = 104.008(8), γ = 94.914(8)°; V = 1653.8 Å^3; Z = 1; ρ_{calcd} = 1.627 g cm^{-1}; $F(000)$ = 784; μ = 5.180 mm^{-1}; T = 293(2) K. An Enraf-nonius CAD-4 diffractometer with graphite-monochromated Mo Kα radiation (λ = 0.710 73 Å) was used. Of 6168 reflections measured ($2\theta_{max}$ = 50.2°) 4666 were observed ($I > 2.0\sigma(I)$). An empirical absorption correction (ψ scan) was applied and the structure solved by Patterson methods and expanded by successive cycles of full-matrix, least-squares refinement on F^2 followed by calculation of a $\Delta\rho$ map. Final refinement on F^2 employed 398 parameters and 33 restraints, the latter being used to maintain known geometry for the solvent acetonitrile and two of the trifluoromethyl groups. The non-hydrogen atoms were refined with anisotropic displacement parameters. Hydrogen atoms were included in calculated positions riding on the attached carbon atoms with isotropic displacement parameters 10% larger than those of the corresponding carbon atoms. R = 0.046 for $I > 2.0\sigma(I)$, and R_w = 0.138 for all data. Goodness of fit S = 1.10 for all observed reflections. Maximum/minimum electron density = 2.19/−1.03 e Å^{-3} (close to Pb atom). All crystallographic calculations were performed with the SHELXTL-PLUS[18] package. Crystallographic data (excluding structure factors) have been deposited with the Cambridge Crystallographic Data Centre as supple-

mentary publication CCDC-149617. Copies of the data can be obtained free of charge on application to the address CCDC, 12 Union Rd., Cambridge CB2 1EZ, U.K. (fax (+44)1223-336-033; E-mail deposit@ccdc.cam.ac.uk).

2. Instrumentation. ^{1}H NMR spectra were obtained using a GE-400 spectrometer (400 MHz). UV−vis spectra were recorded on HP 8452 diode array spectrophotometer. Fluorescence spectra were recorded using a SPEX Fluorolog spectrometer equipped with a 450 W Xe arc lamp for excitation and single grating monochromators with both CCD and thermoelectrically cooled PMT detectors. Spectra were not corrected for detector response. Photolysis experiments were done by irradiation of solutions with a 450 W arc lamp at 356 nm.

3. Materials and Methods. All solvents are of analytical grade and are used without further purification. UV−vis spectra, fluorescence spectra, and ^{1}H NMR spectra of the complexed crown ether derivatives were obtained by adding a concentrated solution of metal ions in acetonitrile (for $CHCl_3/CH_3CN$ systems) or in water (for acetonitrile or acetone systems) to a solution of ligands in either a 1 cm path length cuvette or a 5 mm NMR tube. No more than 10 μL of metal ion solution was added to 3 mL of the measuring solution for fluorescence and UV−vis measurements. For ^{1}H NMR spectral measurements, no more than 10 μL of metal ion solution was added to 0.6 mL of ligand solution. To make batches of obtained results comparable, all samples of metal salts for ^{1}H NMR measurements were dissolved in CD_3CN. The ligand was dissolved in a mixture of $CDCl_3$ and CD_3CN (9:1). In experiments involving Pb^{2+}, $Pb(BF_4)_2$) was dissolved in D_2O and the ligand was dissolved in a mixture of CD_3CN and $CDCl_3$ (3:1). For fluorescence measurements, several solvents such as acetone, acetonitrile, and mixed chloroform−acetonitrile (9:1) were employed, for individual experiments.

4. Stoichiometric Analysis and Stability Constants. The stoichiometric ratios of all the complexes are obtained by the mole ratio method. Changing the mole fraction of the ligand and metal ion through mixing the same concentration of ligand solution and metal ion solution allows one to obtain different fluorescence intensities. Plots of fluorescence intensity vs mole ratio exhibit a maximum at the optimum stoichiometry for the complexes. The ligand **1**−Na^+ complex was determined in a mixture of chloroform and acetonitrile (9:1), and K^+ and Cs^+ were evaluated in acetone. Formation of Pb^{2+} complexes with **2** was examined in pure CH_3CN or CH_3CN/H_2O mixtures. Stoichiometric studies show that all three ligands can form 1:1 complexes (see text) with each alkali metal ion known to form a sandwich complex with the ligand, i.e., **1**−Na^+, **2**−K^+, and **3**−Cs^+.

5. MALDI-TOF Mass Spectra. Mass spectra were obtained using a ThermoBioanalysis LaserMat 2000 MALDI-TOF-MS spectrometer. Spectra were obtained from matrixes formed using 0.5 μL of acetone solution of sample complexes (isolated solid) plus 0.5 μL of saturated α-cyano-4-hydroxycinnamic acid (substance P). Substance P (1348.7, $M^+ + 1$) was added for use as an internal standard.

6. Luminescence Quantum Yields and Time-Resolved Fluorescence Spectra. Quantum yields were determined by using anthracene as standard ($\phi = 0.27$ in polar solvent);[19] corrections were made for small differences in absorption of the sample and reference as shown in the following equation:

$$\phi_{em}{}^{x} = (I_{em}{}^{x}/I_{em}{}^{ref})\phi_{em}{}^{ref}[(1 - 10^{-A_{ref}})/(1 - 10^{-A_x})] \quad (1)$$

Here $I_{em}{}^{x}$ and $I_{em}{}^{ref}$ are the fluorescence intensities, integrated over the emission spectrum of the unknown compound and reference substance, respectively, and A_{ref} and A_x are the absorbance of the reference and the unknown compound at the excitation wavelength. The quantum yields were obtained using an excitation wavelength of 356 nm, the isobestic point in spectrophotometric titrations of the ligands with appropriate alkali metal ions. Fluorescence lifetimes were measured using a PTI LaserStrobe fluorescence lifetime spectrometer with a GL-3300 nitrogen laser (0.04 nm bandwidth, 500 ps pulse width) as an excitation source and stroboscopic detection. The time resolution following deconvolution of experimental decays is 100 ps.

Results

1. Absorption Spectra Associated with Ion Binding. Molecules **1**−**3** have absorption maxima at 382, 390, and 390 nm, respectively, in a mixture of chloroform and acetonitrile (9:1). The polarity of solvent does not affect the absorption maxima significantly because all three compounds have predominantly $\pi \rightarrow \pi^*$ transitions. With the addition of metal ions, i.e., Na^+ to the solution of **1**, K^+ to **2**, and Cs^+ to **3**, only a small blue shift of the absorption maximum is observed. For example, the UV−vis spectral changes observed following addition of CF_3COOK to **2** result in the absorption peak shifting from 390 to 386 nm.

With the addition of 1 equiv of $Pb(ClO_4)_2$ or $Pb(BF_4)_2$ to ligand **2** in CH_3CN, a 16 nm blue shift is observed. Smaller absorption changes result when CF_3COO^- serves as the counterion.

2. Fluorescence Spectra. Unlike the small effect of solvent polarity on the absorption spectra of all three ligands, the luminescence maximum of all ligands red-shifts with increases in solvent polarity. For example, **2** has an emission maximum of 448 nm in chloroform but shifts to 475 nm in acetonitrile with a decrease of quantum yield. With the addition of particular metal ions, all three ligands show significant fluorescence enhancement in solution but their emission behavior is not entirely identical. In acetonitrile, the fluorescence intensity of **2** increases by a factor of nearly 20 upon the addition of a 10-fold molar excess of potassium ion (KSCN aqueous solution). The excitation spectrum of **2** in the absence of K^+ has a maximum at 375 nm; after the addition of an excess of K^+, the excitation maximum shifts to 362 nm, which is consistent with the observed absorption spectral changes following complexation of **2** with K^+. The addition of other alkali metals and alkaline earth metal ions such as Li^+, Na^+, Cs^+, Mg^{2+}, Ba^{2+}, etc., to acetonitrile solutions of **2** does not cause any significant fluorescence change. Only a factor of 1.25 enhancement can be observed from the addition of Na^+, and virtually no change is observed in the emission band shape. The same fluorescence enhancement behavior was observed in acetone. Figure 1 shows emission spectra obtained from **2** with various amounts of added K^+ in mixed solutions of chloroform and acetonitrile (9:1). The inset of Figure 1 shows the fluorescence intensity as a function of the M^+/**2** ratio (M = Na^+, K^+, and Cs^+) monitored at 492 nm. As can be seen, a large fluorescence enhancement is observed with K^+, but Na^+ and Cs^+ do not cause significant fluorescence changes. A small red shift of the emission maximum relative to free **2** is also observed (Table 1).

Solvent clearly plays a large role in the association of ions with ligand **2**. In acetonitrile solution, the saturation point for luminescence of complexed **2** requires more K^+ (>8 equiv), whereas in a mixture of chloroform and acetonitrile (9:1) saturation is reached with slightly more than 1 equiv of K^+. In acetonitrile solutions containing 5% water, K^+ associates with **2** only weakly and Pb^{2+} binds much more effectively than K^+ (vide infra).

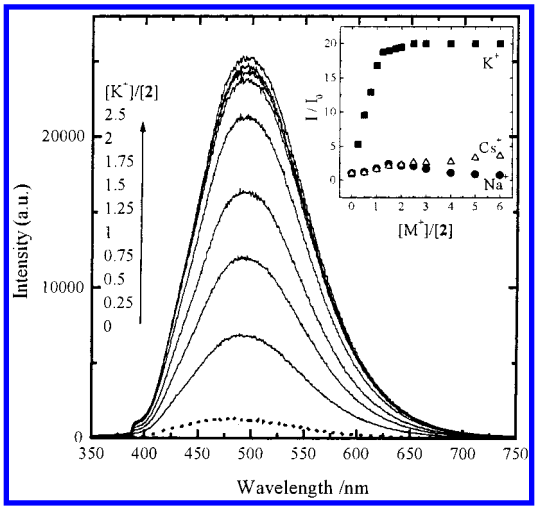

Figure 1. Fluorescence spectral changes of **2** upon addition of K^+ to a mixture of chloroform and acetonitrile (9:1). The inset shows the titration curves of **2** in solution (monitored at 492 nm, excited at 350 nm) when Na^+, K^+, and Cs^+ ions were added. [**2**] = 2.5×10^{-5} M.

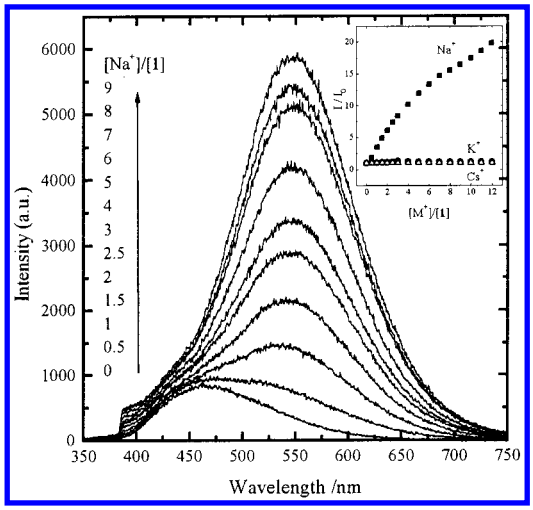

Figure 2. Fluorescence spectrum changes of **1** with the addition of Na^+ in a mixture of chloroform and acetonitrile (9:1). The insert is the titration curves of **1** in solution (monitored at 537 nm, excited at 350 nm) when Na^+, K^+, and Cs^+ ions were added. [**1**] = 2.5×10^{-5} M.

TABLE 1: UV−Vis and Fluorescence Parameters and Stoichiometries in the Mixed Solvent Containing Chloroform and Acetonitrile (9:1)

	ligand						
param	**1**	**1**−Na^+	**2**	**2**−K^+	**2**−Pb^{2+}	**3**	**3**−Cs^+
λ_{max} abs, nm	382	378	390	386	374	390	388
λ_{max} em, nm	462	548	480	492	498	476	512
stoichiometry (M:L)		1:1		1:1	*a*		1:1

[a] For ClO_4^- and BF_4^- the ratio is 1:1; for CF_3COO^- the ratio is 2:1. See text.

Similar fluorescence behavior is observed with **3** in the presence of Cs^+. In acetone solutions of **3**, a significant fluorescence intensity enhancement (factor of ca. 20) is observed upon addition of Cs^+ (CF_3COOCs in acetonitrile or CsF in water). A fluorescence enhancement of a factor of 20 is observed when [Cs^+]/[**3**] is close to 2. This is accompanied by an emission spectral shift from 482 to 526 nm. However, the fluorescence intensity decreases at ratios of [Cs^+]/[**3**] greater than 2. No other alkali metal ions affect the fluorescence of **3** in any significant way, even though K^+ is known to complex with 18-crown-6 very strongly.[2b]

As with the **2**/K^+ adduct, solvent can affect the equilibrium and degree of fluorescence enhancement. In pure acetonitrile solution the fluorescence enhancement for the **3**−Cs^+ adduct is a factor of 4 when the [Cs^+]/[**3**] ratio is less than 2. With further addition of Cs^+ the fluorescence intensity decreases in a way similar to the decrease in chloroform/acetonitrile. More Cs^+ (>8 equiv) is needed to reach the saturation stage in acetone than in chloroform:acetonitrile mixtures (near 2 equiv). Moreover, the fluorescence intensity does not decrease with the addition of excess Cs^+ in acetone, unlike the behavior observed in chloroform/acetonitrile.

Ligand **1**, with a relatively smaller crown ring size, only shows fluorescence enhancement with Na^+ in solution. Figure 2 shows the fluorescence spectral changes when sodium thiocyanate is added. The emission maximum gradually red shifts from around 456 to about 537 nm with the addition of Na^+. The 80 nm red shift is much greater than the 20 nm red shift of **2** with K^+ and the 40 nm red shift for **3** with Cs^+. The inset of Figure 2 shows the titration curves of **1** following addition of Na^+, K^+, and Cs^+ monitored at 537 nm. The fluorescence enhancement based on the integrated emission intensity is much smaller than that of **2** and **3** under the same conditions. Since only a very weak emission can be observed from free **1** around 537 nm, the relative sensitivity for sodium ions monitored at 537 nm is still high enough to distinguish the enhancement resulting from the addition of Na^+. The intensity of the maximum emission at 537 nm is more than 20 times the original fluorescence intensity of the free ligand. Unlike ligands **2** and **3**, in which a small stoichiometric excess can rapidly reach the saturation stage in chloroform /acetonitrile, a much larger amount of Na^+ is required to reach the saturation intensity. Even when the [Na^+]/[**1**] ratio is more than 20, the fluorescence intensity still has not reached its saturation state. The relatively complex behavior observed suggests that more than one luminescent species is formed following complexation of **1** and Na^+. In more polar solvents such as acetone and acetonitrile, **1** does not show any fluorescence enhancement at all when Na^+ is added. It is also found that the anion used can affect the fluorescence behavior of the **1**/Na^+ adduct. When CF_3COONa was used as a cation source, no significant fluorescence enhancement is observed even in chloroform/acetonitrile mixtures.

As stated above, all of the bis-crown ether ligands associate only weakly (or not at all) with alkali metal ions in solutions containing protic solvents. However, it was found that mixed acetonitrile/water solutions (5−10% H_2O) of ligand **2** exhibit a large fluorescence enhancement in the presence of Pb^{2+}. The increase in the emission intensity is accompanied by a shift in the emission maximum from 486 to 498 nm, as shown in Figure 3. The fluorescence intensity at 498 nm is enhanced by a factor of more than 20 times. Interestingly, the plateau of the emission intensity is reached with [Pb^{2+}]/[**1**] ~ 1 when BF_4^- or ClO_4^- are used as anions, but the maximum luminescence enhancement is reached much more gradually with CF_3COO^- as anion which reaches a plateau at a [Pb^{2+}]/[**1**] ratio greater than 4 (inset of Figure 3). Also, $Pb(BF_4)_2$ and $Pb(ClO_4)_2$ give larger fluorescence enhancements than the $Pb(CF_3COO)_2$. Remarkably, no fluorescence enhancement is observed when $Pb(CH_3COO)_2$ is added to acetonitrile solutions of **2**. Other divalent metal ions such as Cu^{2+}, Zn^{2+}, Cd^{2+}, Ni^{2+}, or Co^{2+} do not cause fluorescence enhancement for **2** in aqueous acetonitrile. Only Ca^{2+} and Hg^{2+} induce a slight enhancement of the emission of **2**.

3. Photolysis of Ligands and Complexes. The ligands are all derivatives of distyrylbenzene and, as such, can undergo

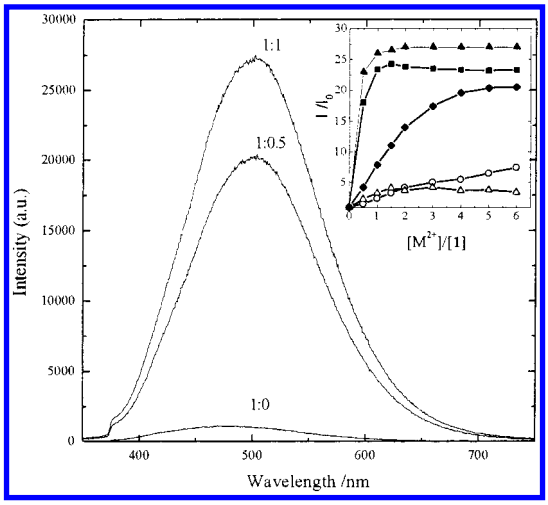

Figure 3. Fluorescence spectral changes of **2** in acetonitrile upon the addition of Pb^{2+}. The inset shows the titration curves of **2** in solution (monitored at 496 nm, excited at 356 nm) upon addition of various metal ions (■, $Pb(BF_4)_2$; ▲, $Pb(ClO_4)_2$; ◆, $Pb(CF_3COO)_2$; ○, Hg^{2+}; △, Ca^{2+}). [**2**] = 1×10^{-5} M.

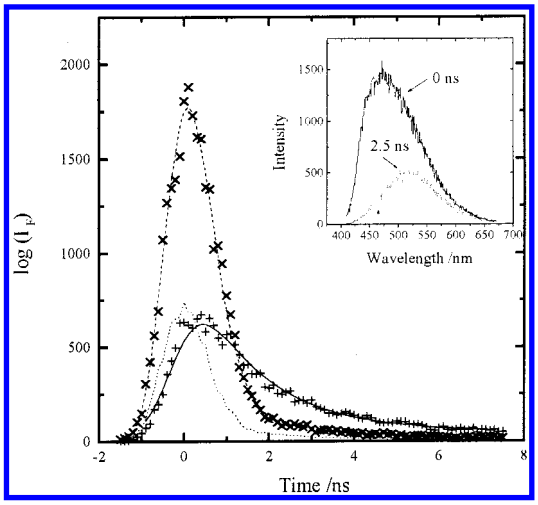

Figure 4. Luminescence decay of **1** and **1** with a 20-fold excess of Na^+ in a chloroform and acetonitrile (9:1). Key: ◆ = scattered laser; × = decay at 455 nm for **1**; + = decay at 535 nm for **1**/Na^+. The inset shows fluorescence spectra of **1**/Na^+ at 0 and 2.5 ns after excitation at 337 nm.

olefin isomerization upon photolysis.[20] Ultraviolet irradiation of solutions of all three free ligands in chloroform at 386 nm results in absorption spectral changes. The absorption at 390 nm decreases and a new peak around 350 nm appears with an isobestic point at 356 nm. This UV−vis spectral change results from the *Z*−*E* (*trans*−*cis*) isomerization. From the absorbency change of the UV−vis spectra, about 40% of the *Z*−*Z* (*trans*−*trans*) isomers is converted to *Z*−*E* (*trans*−*cis*) isomer at steady state following 386 nm irradiation. According to the literature, the closely related cyano-substituted stilbene has two kinds of characteristic proton chemical shifts in ^{1}H NMR.[21] For the *Z* (*trans*-phenyls) isomer, the chemical shift of the proton on the double bond appears at 7.5 ppm, and that of *E* (*cis*-phenyls) isomer is at approximately 7.3 ppm. The ^{1}H NMR spectrum of **2** prior to irradiation exhibits only the peak at 7.5 ppm, indicating that **2** exists exclusively as the *Z*−*Z* (*trans*−*trans*) isomer. Irradiation of the solution of **2** results in the appearance of several new peaks in the aromatic region including a singlet at 7.3 ppm. The ratio of the peak at 7.3 ppm to the peak at 7.5 ppm is 0.63, indicating that there is still about 60% of combined *Z* (*trans*) containing isomers (both *Z*−*Z* and *Z*−*E*) in the irradiated mixture at the photostationary state. This is in accord with the UV−vis spectral changes observed.

It was found that the addition of metal ions to the solutions containing these ligands did not affect the photoisomerization significantly. For example, about 60% *Z*−*Z* (*trans*−*trans*) isomer is present in the ultraviolet-irradiated $CHCl_3/CH_3CN$ (9:1) solutions of **2** containing excess K^+. When either solutions of **2** or a solution containing **2** and K^+ are irradiated at 386 nm, the fluorescence intensity decreases but the emission maximum remains unchanged.

4. Luminescence Quantum Yields and Time-Resolved Fluorescence Measurements. In polar solvents, such as acetone and acetonitrile, emission quantum yields of **1**−**3** are all low (about 0.001) relative to alkyl-substituted disytrylbenzene derivatives.[20] However, the quantum yields of the ligands are larger in less polar or nonpolar solvents. Table 2 shows the quantum yields of ligand **1**−**3** together with the complex with Na^+, K^+, and Cs^+, respectively. Also included is the luminescence yield of ligand **2** in aqueous acetonitrile solutions in the presence of Pb^{2+}. Complex quantum yields were measured for the ratio of metal ion to ligand that gave the largest luminescence enhancement.

TABLE 2: Quantum Yield, Lifetime and Radiative Kinetic Constants of 1−3 and Their Complexes in the Mixed Solvent of Chloroform and Acetonitrile (9:1)

compd	ϕ_{Fl}	τ (ns)	k_r (s^{-1})
1	0.007	0.1	7.0×10^7
1−Na^+	0.06	0.7, 2.4	$2.5 \times 10^{7\,a}$
2	0.011	0.1	1.1×10^8
2−K^+	0.28	1.0	2.7×10^8
3	0.011	0.12	9.2×10^7
3−Cs^+	0.17	1.5	1.1×10^8
2−Pb^{2+}	~0.2[b]		

[a] k_r calculated from the longer lifetime component. [b] In mixed CH_3CN-H_2O (9:1).

The lifetimes of all the ligands together with their complexes are listed in Table 2. It was found that the lifetime for free **2** is approximately 0.1 ns in $CHCl_3-CH_3CN$ (9:1). Upon addition of K^+, the lifetime increases, reaching a value of 0.98 ns at [K^+]/[**2**] = 1.0. The radiative decay rate constant determined from the quantum yield and lifetime does not change significantly and is approximately 1×10^8 s^{-1}.[22] Time-resolved fluorescence spectra of **2** following addition of K^+ indicate that there is virtually no spectral shift at different time delays for solutions containing different ratios of [K^+]/[**2**].

For free **3**, the lifetime is about 0.12 ns and it increases to 1.5 ns when the ratio of [Cs^+]/[**3**] is greater than 1. It is interesting to note that the lifetime does not change when more than 2 equiv of Cs^+ is added whereas the steady-state fluorescence intensity decreases. Similar to the spectral changes in the **2**/K^+ complex formation, no spectral change is observed at different delay times.

The behavior of **1**, however, differs significantly. Time-resolved emission spectra reveal that a red shift occurs following excitation and that the emission decay consists of two components. In the absence of Na^+ the luminescence of **1** is monoexponential. The lifetime of the free **1** is about 0.1 ns; as Na^+ is added the decay becomes double exponential, with components of 0.8 and 2.4 ns. The relative contribution of the long-lived component of the decay increases gradually as the [Na^+]/[**1**] ratio increases until a stable value is reached with a 15-fold excess of Na^+. Time-resolved fluorescence spectra, shown in Figure 4, indicate that the fluorescence emission peak red-shifts from 460 to 540 nm after excitation of solutions having [Na^+]/[**1**] = 20.

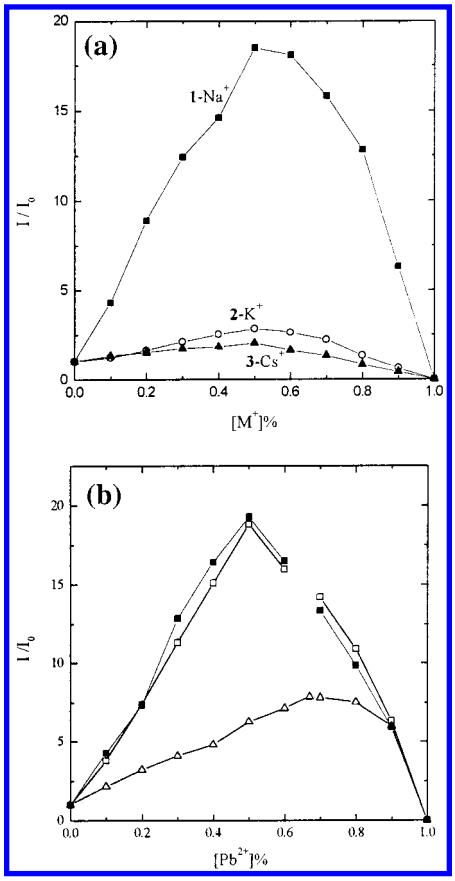

Figure 5. Fluorescence intensity changes (a) of **1** (■), **2** (○), and **3** (▲) with the mole fraction Na^+, K^+, and Cs^+, respectively, in CH_3CN ([**2**] = [**3**] = 2.5×10^{-5} M; [**1**] = 2.5×10^{-3} M) and (b) of **2** in CH_3CN-H_2O (95:5) with mole fraction of Pb^{2+} ([**2**] = 5.48×10^{-5} M; $Pb(BF_4)_2$ (■); $Pb(ClO_4)_2$ (□); $Pb(CF_3COO)_2$ (△)).

5. Stoichiometric Analysis and Ion Competition. The stoichiometry of the alkali metal ion/ bis-crown complex can be evaluated from the fluorescence intensity as a function of the mole fraction of each species using a Job's law approach. Figure 5a shows the ratio of the fluorescence intensity vs mole fraction of alkali metal ion for all three ligands with each of the alkali metal ions. It was found that all three ligands form bis-crown/alkali metal ion complexes with overall 1:1 stoichiometry. In each case, there are two crown rings/metal ion. Given 1:1 stoichiometry, the association is consistent with the formation of two sandwich complexes involving two bis-crown ligands and two alkali metal ions (since intramolecular sandwich complex formation is not possible for the bis-crown). In fact, the concentration dependence of the emission intensity (insets of Figures 1−3) can be fit to either 1:1 or 2:2 equilibrium expressions as shown in eq 2. The data could not be fit using other possible stoichiometries, such as 1:2 M^+:L. From the analysis of fluorescence titration data, the **2**/K^+ complex and **3**/Cs^+ complexes qualitatively appear to have higher stability constants than the **1**/Na^+ complex in 9:1 chloroform−acetonitrile.

$$M^+ + L \leftrightharpoons ML^+ \qquad (2)$$

$$2M^+ + 2L \leftrightharpoons M_2L_2^{2+}$$

Ratiometric studies of luminescence enhancement indicate that **2** forms 1:1 complexes with $Pb(BF_4)_2$ and $Pb(ClO_4)_2$, similar to the complexes of **2** with K^+ and **3** with Cs^+, indicating each

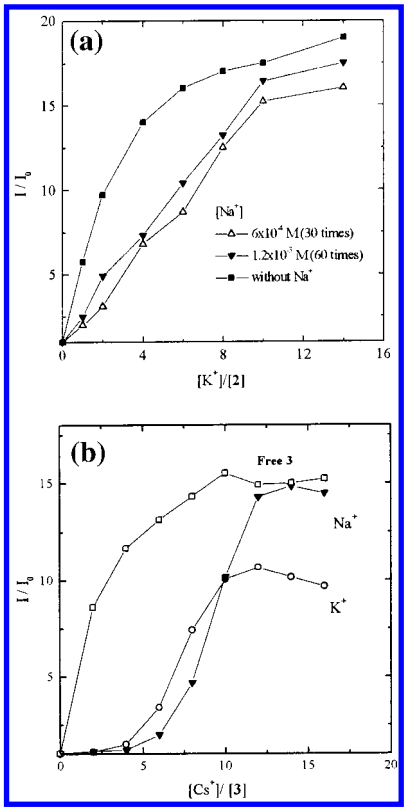

Figure 6. (a) 492 nm fluorescence intensity changes of **2** upon the addition of K^+ ion to acetonitrile solutions containing Na^+ ([Na^+] = 0 M (■), 6×10^{-4} M (△), and 1.2×10^{-3} M; [**2**] = 2×10^{-5} M). (b) Fluorescence intensity changes of **3** upon the addition of Cs^+ ion to acetone solutions containing K^+ or Na^+ ([K^+] = 3.75×10^{-4} M, [Na^+] = 3.75×10^{-4} M). The emission intensity was monitored at 526 nm. [**3**] = 2×10^{-5} M.

Pb^{2+} ion associates with two 15-crown-5 rings when ClO_4^- and BF_4^- are used as counteranions. However, with CF_3COO^- as the counteranion, **2** forms a 2:1 Pb^{2+}:**2** complex in acetonitrile. Figure 5b shows the emission intensity as a function of the mole ratio at fixed total concentration, clearly indicating the stoichiometry of the Pb^{2+}/**2** complex for each of the three counterions. An explanation of this difference in stoichiometry is provided by the X-ray crystal structure of this complex (vide infra).

The degree of fluorescence enhancement was examined for each of the pairs of chromophores and alkali metal ions in the presence of competing ions. Figure 6a shows the fluorescence intensity changes as a function of added K^+ when varying excesses of Na^+ (30−60 times) are present in acetonitrile solutions containing **2**. It was found that Na^+ only slightly perturbs the response from K^+. Regardless of the Na^+ concentration, the fluorescence intensity increases gradually to reach the saturation level. While it can be seen that the fluorescence enhancement from K^+ in the presence of Na^+ is lower than that of the solution without Na^+, it is clear that potassium ions can displace Na^+ from the **2**/Na^+ complex.

Similar results are obtained for Cs^+ and ligand **3** in the presence of both Na^+ and K^+. Figure 6b shows the fluorescence intensity changes upon the addition of Cs^+ to the acetone solution of **3** when either K^+ or Na^+ is present. Although both K^+ and Na^+ cause some interference of the fluorescence response, the fluorescence is turned on when [Cs^+]/[K^+] or [Cs^+]/[Na^+] reaches ca. 1:4.

In CH_3CN-H_2O (95:5) the only ions that cause a fluorescence change in ligand **2** are Pb^{2+} and Ca^{2+}. The presence of Ca^{2+} alone causes some perturbation to the fluorescence

CHART 1

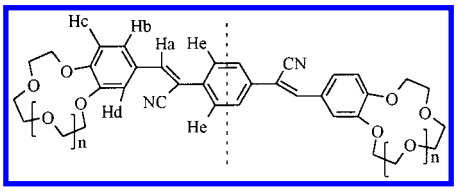

TABLE 3: Assignment of the Chemical Shifts of Aromatic Protons in ^{1}H NMR Spectra of 1−3 in $CHCl_3$

ligand	H_a	H_b	H_c	H_d	H_e
1	7.49 (1)	7.46 (1)	6.99 (1)	7.68 (3)	
2	7.48 (1)	7.35 (1)	6.87 (1)	7.62 (1)	7.66 (2)
3	7.48 (1)	7.35 (1)	6.87 (1)	7.63 (1)	7.67 (2)
2[a]	7.69 (1)	7.48 (1)	6.98 (1)	7.64 (1)	7.75 (2)

[a] In $CD_3CN-CDCl_3$ (3:1).

response, as seen from the inset in Figure 3. Despite the fact that Ca^{2+} binds to **2**, titration curves of Pb^{2+} in solutions containing **2** with 100- and 300-fold excesses of Ca^{2+} are essentially unaffected by the presence of the competing ion.

6. ^{1}H NMR Spectra. Since all three chemosensor molecules have a 2-fold symmetry axis, the assignment of all the protons in the molecule was relatively simple. Chemical shifts for all the aromatic protons (shown in Chart 1) are listed in Table 3.

Protons H_e, H_b, and H_d appear at relatively low field due to the deshielding caused by the ring current of cyano group. It is interesting that, in the absence of added alkali metal ions, the order of the chemical shifts of the aromatic protons of **1**−**3** are not identical. For **1**, protons H_b and H_c are further downfield than the same resonances in **2** and **3** by approximately 0.1 ppm while proton H_d merges with H_e in **1**, approximately 0.05 ppm downfield relative to compounds **2** and **3**. Overall, the aromatic resonances are well separated and the coupled protons are all AX. The single most important qualitative observation relating to alkali metal ion incorporation is that significant (0.1−0.3 ppm) chemical shift changes occur for the aromatic resonances of **1**−**3** *only* in the presence of Na^+, K^+ (or Pb^{2+}), and Cs^+, respectively.

Distinct changes in the ^{1}H NMR aromatic resonances occur for all three ligands, making examination of alkali metal ion complexation possible. Figure 7a shows that the aromatic proton resonances of **1** shift in frequency significantly upon addition of NaSCN. All aromatic protons shift upfield except for H_a, which exhibits a small downfield shift. The progressive shift in the resonances with increasing Na^+ concentration suggests exchange of the Na^+ ions between different crowns is fast on the NMR time scale.[23] The aromatic chemical shift changes as the molar ratio of [Na^+]/[**1**] is increased until about 4 equiv of Na^+ is added. Large upfield shifts, approximately −0.2 ppm, are observed for H_d and H_e. The downfield shift of H_a is about 0.04 ppm. The aliphatic resonances, associated with the crown, exhibit only broadening after 1 equiv of Na^+ is added. Previously, we found that CF_3COONa did not cause any fluorescence enhancement in CH_3CN. Consistent with this, only very small chemical shifts (−0.01 to ∠0.03 ppm) were observed for all the protons in **1** following the addition of CF_3COONa.

Ligand **2** exhibits entirely different ^{1}H NMR spectral changes upon the addition of K^+, as shown in Figure 7b. On the basis of the chemical shift differences observed for **1** in the presence of Na^+, the resonances at 7.62 and 7.66 (H_d and H_e) disappear and new resonances appear at 7.34 and 7.28 ppm. The new peak at 7.21 ppm corresponds to H_b of free **2**. The behavior differs from that of the Na^+/**1** complex in that the spectral changes indicate exchange of K^+ is slow on the NMR time scale. Aside from the significant changes of chemical shifts of aromatic protons, the aliphatic protons show considerable broadening. Similar ^{1}H NMR spectral changes are observed when either the thiocyanate or trifluoroacetate salts are used. No significant aromatic chemical shift changes are observed when CF_3COONa is added to solutions of **2**, despite the fact that benzo-15-crown-5 is known to bind Na^+.

When cesium trifluoroacetate is added to solutions of **3**, the ^{1}H NMR spectra exhibit changes that differ from those of **1** with Na^+ and **2** with K^+. The ^{1}H NMR spectral changes in the aromatic region are shown in Figure 7c. The difference is most easily seen for proton H_c which exhibits an upfield shift at Cs^+:**3** ratios less than 2; the addition of further Cs^+ results in a downfield shift of the resonance. This reverse in the direction of the chemical shift for the protons of **3** occurs over the same concentration range as the falloff in the fluorescence of solutions containing **3** and Cs^+. Significant broadening of the peaks H_d and H_e is observed when a small amount of Cs^+ is added to $CDCl_3$ solutions of **3** ([Cs^+]/[**3**] = 0.25). With the addition of more Cs^+, new peaks appear upfield of the noncoordinated H_d and H_e resonances. As with the other complexes, the peaks corresponding to the aliphatic region are broadened upon addition of Cs^+ ion.

Studies of the interaction between CF_3COOK and **3** by ^{1}H NMR show that all aromatic protons shift downfield about 0.02−0.04 ppm without noticeable broadening of the resonances. Since K^+ is known to coordinate to a single benzo-18-crown-6, the spectral differences observed indicate that the mode of coordination is completely different for association of **3** with Cs^+ ion.

Figure 8a shows the ^{1}H NMR spectral changes upon addition of $Pb(CF_3COO)_2$ to a mixture of CD_3CN/CD_3Cl (3:1). It was found that H_a, H_d, and H_e show significant downfield shifts while other protons, H_b and H_c, shift upfield. The spectral changes resemble those of **2** with K^+. Unlike the relatively simple changes observed upon formation of the adduct between **2** and $Pb(CF_3COO)_2$, the ^{1}H NMR spectra obtained following addition of $Pb(BF_4)_2$ and $Pb(ClO_4)_2$ are very different. In both cases many new peaks appear in the aromatic region upon addition of these salts; the spectrum for $Pb(ClO_4)_2$ is shown in Figure 8b. All peaks shift upfield upon coordination to Pb^{2+}.

In principle, the ^{1}H NMR data could be used to determine equilibrium constants for metal ion association with the different bis-crown ligands using various models. Given that the fluorescence titration data, obtained at much lower concentrations of ligand, fit both 1:1 (one more of M^+/mol of ligand) or 2:2 association equilibria (eq 2), attempts were made to simulate the observed aromatic spectral changes for particular resonances. For instance, the chemical shift changes observed for proton H_e of ligand **1** upon addition of Na^+ were simulated by assuming metal ion exchange was much faster than the relaxation time of either the free or coordinated protons. The spectra obtained could not be simulated assuming either a 1:1 or 2:2 (or any other) association equilibrium model for the above case or any other ion/ligand combination. Thus, while the very simple changes observed in the NMR spectra for Na^+/**1**, K^+/**2**, and Cs^+/**3** suggest there exist only two predominant species in solution (free ligand or sandwich structure resulting in perturbation of aromatic resonances), the concentration dependence of the observed spectral changes suggests that sandwich formation leads to a variety of species in solution.

7. MALDI-TOF Mass Spectra. Complexes of the ligands with different alkali metal ions were also examined by matrix

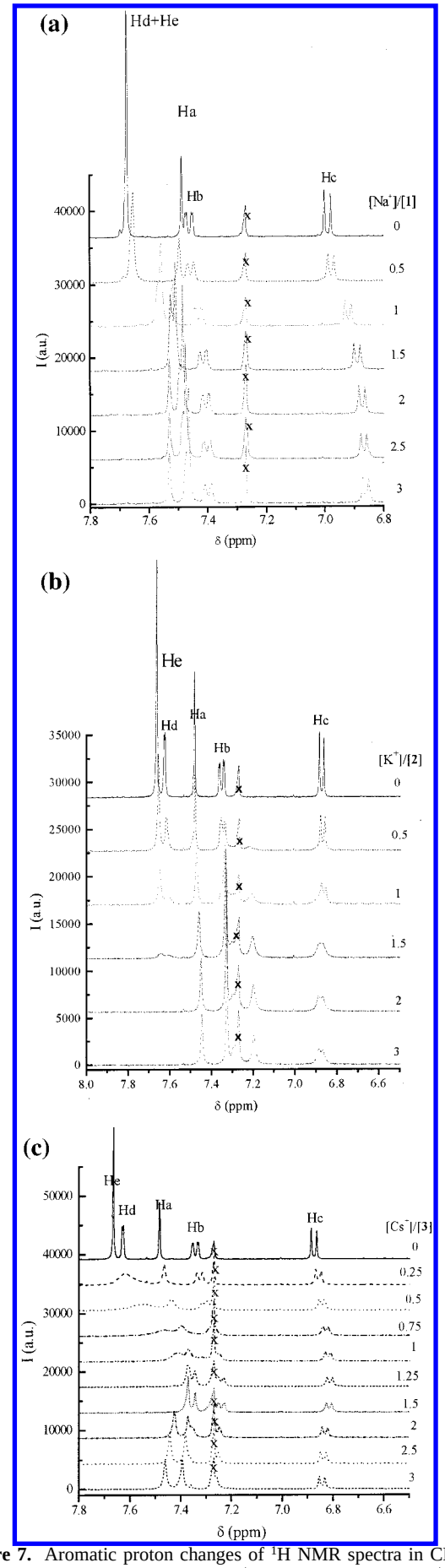

Figure 7. Aromatic proton changes of ^{1}H NMR spectra in $CDCl_3-CD_3CN$ (9:1) at different ratios of M^+ to L (5 mM) for (a) Na^+ added to **1**, (b) K^+ added to **2**, and (c) Cs^+ added to **3**.

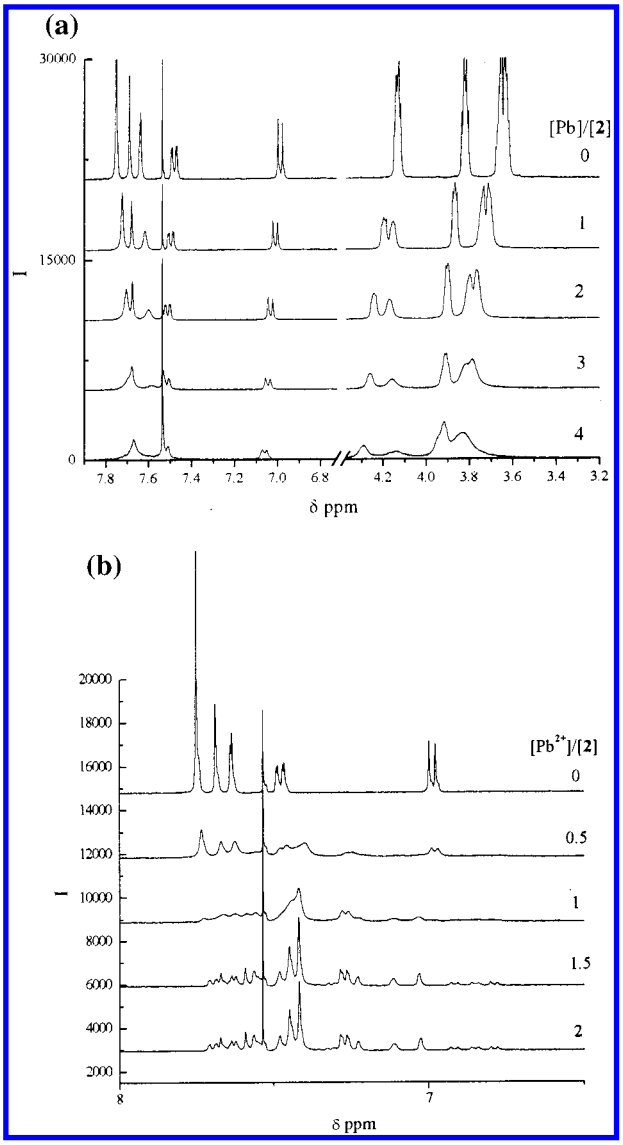

Figure 8. ^{1}H NMR spectral changes observed upon addition of (a) $Pb(CF_3COO)_2$ and (b) $Pb(ClO_4)$ to **2** (5 mM) in a mixture of CD_3CN-CD_3Cl (3:1).

TABLE 4: MALDI-TOF Mass Spectral Data for Different Complexes with Numbers in Parentheses Being Molecular Weights Calculated for the Species Noted at the Top of the Column

complex	L	LM^+ or $L_2M_2^{2+}$	L_2M^+
1$-Na^+$	628 (624)	651 (647)	1279 (1271)
2$-K^+$	714 (712)	752 (751)	1471 (1463)
2$-Na^+$	713 (712)	736 (735)	1447 (1447)
3$-Cs^+$	804 (800)	938 (932)	

assisted laser desorption and ionization time-of-flight mass spectroscopy (MALDI-TOF). Table 4 shows the principal ions obtained for different ion/ligand combinations. For the complex of **1** with Na^+, a peak centered at a mass of 628, corresponding to the free **1** (fw 624), was observed. The observed masses represent peaks in the MALDI-TOF spectra and are therefore averaged masses including ions with heavier isotopes; as a result, the observed masses are higher than those calculated for particular ions. Two other peaks, at *m*/*e* 651 and 1279, correspond to **1**/Na^+ (fw 647) and $\mathbf{1}_2/Na^+$ (fw 1271) adducts, respectively. For the complex of **2** and K^+, similar results were obtained. The peaks observed appeared at 714, 752, and 1471 corresponding to free **2** (fw 712), **2**/K^+ (fw 751), and $\mathbf{2}_2/K^+$

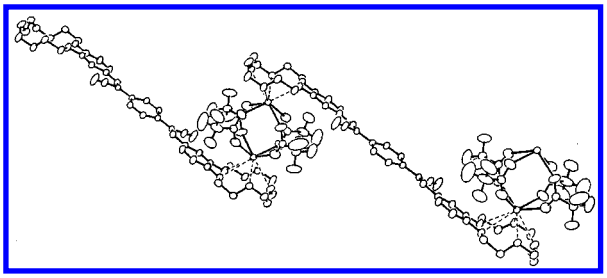

Figure 9. Structure of crystalline adduct of **2** with $Pb(CF_3COO)_2$ showing $Pb_2(CF_3COO)_4$ units bridging 15-crown-5 moieties of two **2** molecules.

(fw 1463), respectively. It should be noted that the peak at *m*/*e* 647 of **1**/Na^+ complex and the peak at *m*/*e* 752 of **2**/K^+ could also be attributed to the double-sandwich species $[Na_2/\mathbf{1}_2]^{2+}$ and $[K_2/\mathbf{2}_2]^{2+}$; the MALDI-TOF technique cannot distinguish the two species since mass resolution better than 1 amu is required for both the **1**-Na^+ adduct and **2**−K^+ adducts. No peak representing $[Na_2/\mathbf{1}_2]^{2+}$ or $[K_2/\mathbf{2}_2]^{2+}$ together with a single counterion was observed.

Since Na^+ is known to coordinate with 15-crown-5 (i.e. **2**), the Na^+/**2** complex was also examined. Peaks at *m*/*e* 713 and 736 were observed, corresponding to the free ligand of **2** (fw 712) and **2**/Na^+ complex (fw 735). Two other peaks at *m*/*e* 885 and 1448 were attributed to **2**/$CF_3CO_2Na/Na(H_2O)^+$ (fw 889) and $\mathbf{2}_2/Na^+$ (fw 1447).

For the complex of ligand **3** with Cs^+, besides the peaks at *m*/*e* 804 and 938 from free **3** (fw 800) and **3**/Cs^+ (fw 932), two other peaks at *m*/*e* 1200 and 1629 were also observed. The *m*/*e* 1200 peak may come from **3**/$CF_3CO_2Cs/Cs(H_2O)^+$ (fw 1197) similar to the ones seen in the **2**/Na^+ complex system.

8. Crystal Structure of $Pb(CF_3COO)_2$ Adduct with 2. We were able to prepare crystals of the **1**/$Pb(CF_3COO)_2$ complex suitable for crystallographic analysis. Figure 9 shows the crystal structure of the **1**/$Pb(CF_3COO)_2$ adduct precipitated from acetonitrile solutions. It was found that the complex is composed of an alternating sandwich structure in which lead links the bis-crown ligands together in a stair step progression. Each sandwich of the complex molecule contains two lead atoms linked by four bridging trifluoroacetate anions. The coordination number of each lead in the structure is 9. On average, one ligand associates with two lead ions, in agreement with the solution stoichiometric results. The distance between the two Pb atoms in the tetrakis(μ-CF_3COO) bridge is 4.52 Å, and the distance between the two ligands in one unit (the mean plane of two crown rings) is approximately 8.2 Å. Each distyrylbenzene unit of the packed solid overlaps partially with a distyrylbenzene on a neighboring stair. The closest distance between two adjacent sandwich layers (π-plane spacing) is 3.5−3.6 Å.

Discussion

It is known that Na^+ can form sandwich compounds with 12-crown-4;[24] this results from the fact that the ionic radius of Na^+ is larger than the cavity of 12-crown-4. Similar results have been obtained for 15-crown-5 with K^+ [25] and 18-crown-6 with Cs^+.[26] From the stoichiometric fluorescence analysis, all the ligands form 1:1 complexes; i.e., on average one molecule of ligand (with two crowns) coordinates to one metal ion. The MALDI mass spectral data clearly show the presence of sandwich complexes since ions are observed for stoichiometries involving two bis-crowns and one alkali metal ion. In addition, the ^1H NMR results indicate that significant chemical shift changes of the aromatic resonances occur *only* for alkali metal ion/bis-crown combinations that exhibit large fluorescence enhancements (i.e. Na^+ + **2**). The structure of the $Pb(CF_3COO)_2$/**2** adduct clearly illustrates formation of an extended sandwich structure, although the stoichiometry differs from that of the alkali metal ion/bis-crown complexes. The similarity of the large ^1H NMR shifts of the aromatic protons for the $Pb(CF_3COO)_2$/**2** adduct and the complexes of **1**−**3** with Na^+, K^+, and Cs^+, respectively, suggests the solution structures in all of the strongly luminescent species formed are related. Previously, Kleinpeter et al.[27] studied a relatively rigid bis-15-crown-5 Shiff-base molecule of 1,4-bis(((2,3,5,6,8,9,11,12-octahydro-1,4,7,10,13-tetraoxabenzopentadecen-15-yl)m ethylidene)amino)benzene by ^1H and ^{13}C NMR spectroscopy. They suggested that a "pocket complex", i.e., an intramolecular sandwich structure, was formed with K^+. Lockheart et al.[28] recently used ^{13}C NMR to study a relatively more flexible molecule in which two benzo-15-crown-5 rings were linked by propanediamine. They found that both intermolecular and intramolecular sandwich structures were formed in solution. Wang and co-workers obtained the crystal structure of another rigid Shiff-base complex of *N*,*N*′-(*m*-phenylenedimethylidyne)bis(3,4-(1,4,7,10,13)-pentadeceno)-aniline with potassium picrate. The structure revealed that discrete *2*:*2 sandwich structures can be formed*.[29] The idea that *extended* sandwich structures are involved in the luminescent enhancements observed here is also supported by results for ligand **4**; with only a single crown on the chromophore, no luminescent enhancement is observed in the presence of K^+, the ion capable of forming sandwich complexes with the crown. The discussion below provides evidence for formation of extended sandwich structures for complexes of **1** with Na^+, **2** with K^+ (and Pb^{2+}), and **3** with Cs^+.

From the MALDI mass spectral results presented here, a sandwich structure with two ligands and one metal ion is observed in all the cases, namely, $\mathbf{1}_2/Na^+$, $\mathbf{2}_2/K^+$, and even $\mathbf{2}_2/Na^+$. In addition 1:1 complexes such as **1**/Na^+, **2**/K^+, and **3**/Cs^+ are also observed. The 2:2 sandwich structures such as $[Na_2/\mathbf{1}_2]^{2+}$, $[K_2/\mathbf{2}_2]^{2+}$, $[Cs_2/\mathbf{3}_2]^{2+}$, or $[Na_2/\mathbf{3}_2]^{2+}$ cannot be definitively assigned by MALDI since the charge-to-mass ratio is the same as the 1:1 complexes; better than unit mass resolution is required to distinguish two types of structures.

Proton NMR data further support the formation of sandwich structures for the strongly luminescent complexes formed. The metal free form of all three ligands is exclusively the *Z*−*Z* (*trans*−*trans*) isomer. In this isomer, H_b, H_d, and H_e can be affected by the electronic current of the cyano group if some degree of stacking of the aromatic structures occurs upon sandwich complex formation. When appropriate alkali metal ions are added, large chemical shift changes occur for **1** with Na^+, **2** with K^+, and **3** with Cs^+, particularly for protons H_d and H_e. In addition, only very small changes in the aromatic resonances are observed for complexes of **2** with Na^+ and **3** with K^+, where coordination of the ions involves intercalation. Sandwich formation can lead to complexes such as those found by others (discrete 2:2 complex observed by Wang and co-workers)[29] or oligomeric species resulting from sandwich formation (similar to the Pb^{2+} complex with **2**). In addition, the simplicity of the NMR spectral changes observed suggests that single sandwich structures (i.e. two molecules of **1** with a single Na^+ bound to one crown of each ligand) are not present in significant concentration.

Complex formation between Pb^{2+} and **2** in acetonitrile is dependent on the counterion. With CF_3COO^- as counterion, fluorescence results indicate that **2** forms a 1:2 **2**:Pb^{2+} complex in acetonitrile. ^1H NMR spectra, however, are similar to those

obtained for complexation of **2** and K^+ where fluorescence titration data yields a 1:1 stoichiometry. The crystallographic data presented here illustrate a sandwich structure formed between $Pb_2(CF_3COO)_4$ units and two 15-crown-5 moieties of **2**, yielding an overall 1:2 **2**:Pb^{2+} stoichiometry. In solutions containing **2**, Pb^{2+}, and either ClO_4^- or BF_4^-, 1:1 complexes are formed, and ^{1}H NMR spectra differ markedly from those of the other sandwich complexes formed. The spectra obtained at Pb^{2+}:**2** ratios of 2 or greater clearly show that the 2-fold symmetry of the ligand has been broken, indicating an asymmetry in the coordination environment of the two 15-crown-5 ligands of **2**. In this case the 1:1 overall stoichiometry observed in fluorescence titrations supports simple crown structures involving coordination of two 15-crown-5 rings with one lead ion; crystallographic results of Dehnicke et al. indicate the formation of a simple sandwich of 15-crown-5 with Pb^{2+} is possible.[30] We are currently attempting to isolate crystals of the adduct formed between **2** and Pb^{2+} in the presence of either ClO_4^- or BF_4^- in an effort to better understand the relationship between the solution ^{1}H NMR and luminescence behavior.

As stated in the results, evidence from both UV−vis and ^{1}H NMR indicates that spectral shifts occur upon irradiation. These results indicate that all three ligands undergo photoinduced *Z*−*E* (*trans*−*cis*) isomerization. However, there is still more than 60% *Z*−*Z* (*trans*−*trans*) isomer present at the photostationary state. When K^+ is added to **2** and the solution is irradiated**,** photoisomerization occurs to yield a steady state having approximately 60% of *Z*−*Z* (*trans*−*trans*) isomer, nearly the same as the free ligand. Since the fluorescence yields of free ligand **2** and K^+/**2** are 0.011 and 0.22, the majority of the decay of both complexes is nonradiative (including, but not limited to, the isomerization of the *Z*−*Z (trans*−*trans)* isomer). Luminescence lifetime data illustrate that formation of the alkali metal ion complexes results in longer emission lifetimes. This, coupled with the increase in the emission quantum yield, indicates the change in luminescence intensity results from a decrease in the nonradiative decay rate constant for the K^+ and Cs^+ complexes (k_r is not significantly changed).

All the luminescence decays obtained appear to be single exponential with the apparatus used. This is surprising since exposure to light induces isomerization to yield a significant amount of the *Z*−*E* (*trans*−*cis*) isomer; even assuming all the *Z*−*Z* (*trans*−*trans*) isomer of the ligand (either **1** or **2**) is bound to the appropriate alkali metal ion, luminescence from the *Z*−*E* (*trans*−*cis*) isomer should be observed. Sandros and co-workers conducted a detailed examination of the photophysics of the isomers of a distyrylbenzene derivative.[20] They found that the *Z*−*E* (*trans*−*cis*) and *E*−*E* (*cis*−*cis*) isomers have much lower emission quantum yields and lifetimes than the *Z*−*Z* (*trans*−*trans*), perhaps by as much as a factor of 100. If comparable differences exist for these compounds, it is conceivable that the luminescence decay of the *Z*−*E* (*trans*−*cis*) and *E*−*E* (*cis*−*cis*) isomers may occur on a time scale short relative to the excitation profile of the laser source used for lifetime analysis in this work. Thus, the observation of single exponential decays is possible given this precedent for excited-state decay of derivatives containing the *E* isomer. The formation of either discrete 2:2 ligand−alkali metal ion complexes (rectangles) or extended sandwich linked oligomeric structures that serve to inhibit isomerization of the excited state is consistent with the observed change in the photophysical behavior. It is well-known that the main path of nonradiative deactivation of the lowest excited singlet state of stilbene is via rotation about the ethylenic double bond.[31] Inhibiting bond rotation in stilbene results in enhanced fluorescence emission in solid matrixes,[32] viscous solvents,[33] and cyclodextrin inclusion complexes.[34] In this system, formation of sandwich complexes at both the crowns of the ligand may lead to more rigid complexes having very high activation barriers to rotation in the excited state. This type of effect is believed to explain the behavior observed by Shinkai. et al. for stilbene−boronic acid derivatives used for sensing disaccharides in aqueous solution.[35]

The **1**/Na^+ complex exhibits a nearly a 10-fold decrease in k_r relative to free **1**, suggesting the nature of the longer lived emitting species differs from that of **2**/K^+ and **3**/Cs^+. Additionally, time-resolved luminescence spectra clearly show that the spectrum obtained immediately after excitation has a maximum at much shorter wavelengths than the spectrum obtained after a few nanoseconds (Figure 4). Further, the luminescence decay of solutions containing **1** and Na^+ are double exponential with lifetimes of $\tau = 0.7$ and 2.4 ns. An explanation for this behavior is that the two components correspond to two different **1**/Na^+ complexes in solution; the red-shifted longer decay may represent excimer emission from the two chromophores of stacked sandwich complexes. The possibility of excimer emission depends on the orientation and separation of the two distyrylbenzene chromophores in the double-sandwich complex. It is certainly reasonable that the double-sandwich complex of ligand **1** with Na^+ has a smaller ligand−ligand separation than the (**2**/K^+)$_2$ or the (**3**/Cs^+)$_2$ complexes since Na^+ has the smallest ionic radius.

Summary

This work illustrates the development of chemosensors based on fluorescence enhancement through the formation of extended sandwich structures. Sensor molecules **1**−**3**, each with a different crown ring size, respond to Na^+, K^+, and Cs^+ selectively in aprotic solvents, and **2** binds Pb^{2+} in aqueous acetonitrile solutions. The Pb^{2+} complex with **2** forms a unique structure involving a $Pb_2(CF_3COO)_4$ unit sandwiched between two crown moieties of **2** ligands. The Pb^{2+} complex and the other complexes exhibiting strong fluorescence all have mass spectra indicating sandwich formation and unique spectral changes in ^{1}H NMR that differ from spectra obtained for simple ion intercalation. The fact that the ligand with a single crown, **4**, exhibits no fluorescence enhancement in the presence of the ion leading to sandwich formation further supports the idea that extended multisandwich structures are formed that involve both crowns of multiple ligands. These extended structures lead to a decrease in observed nonradiative relaxation rate constants for individual chromophores and, thus, much higher fluorescence yields. Competition experiments indicate that both sensors **2** and **3** have relatively high selectivity for K^+ and Cs^+, respectively, in the presence of other alkali metal ions; we are currently exploring potential application of these chemosensors in solution environments where ion competition is an important consideration.

Acknowledgment. The authors wish to thank the U.S. Office of Naval Research through the Tulane Center for Bioenvironmental Research for the support of this work. This work was supported in part also by the Office of Basic Energy Sciences of the U.S. Department of Energy. This is document NDRL-4349 from the Notre Dame Radiation Laboratory.

References and Notes

(1) Eggins, B. *Biosensors*: *An introduction*; John Wiley and Sons: Chichester, U.K., 1996.

(2) For example: (a) Kimura, K.; Shono, T. In *Cation Binding by Marcrocycles Complexation of Cationic Species by Crown Ethers*; Inoue, Y., Gokel, G., Eds.; Marcel Dekker: New York, 1990. (b) Buhlmann, P.; Pretsch, E.; Bakker, E. *Chem. Rev.* **1998**, *98*, 1593.

(3) Masilamani, D.; Lucas, M. E. In *Fluorescent Chemosensors for Ion and Molecule Recognition*; Czarnik, A. W., Ed.; American Chemical Society: Washington, DC, 1992.

(4) See review: de Silva, A. P.; Gunaratne, H. Q. N.; Gunlaugsson, T.; Huxley, A. J. M.; McCoy, C. P.; Rademacher, T. T.; Rice T. E. *Chem. Rev.* **1997**, *97*, 1515.

(5) (a) An, H. Y.; Bradshaw, J.; Izatt, R. M.; Yan Z. *Chem. Rev.* **1994**, *94*, 939. (b) Izatt, R. M.; Bradshaw, J. G.; Pawlak, K.; Bruening, R. C.; Tarbet, B. J. *Chem Rev.* **1992**, *92*, 1261. (c) Sutherland, I. O. In *Advances in Supramolecular Chemistry*; Gokel, G. W., Ed.; JAI Press: Greenwich, CT, 1990; Vol.1, pp 65−108. (d) Hancock, R. D.; Martell, A. E. *Chem Rev.* **1989**, *89*, 1875.

(6) For example: (a) Bourson, J.; Valeur, B. *J. Phy. Chem.* **1989**, *93*, 3871. (b) Letard, J. F.; Lapouyade, R.; Retting, W. *Pure Appl. Chem.* **1993**, *65*, 1705.

(7) For example: (a) Czarnik, A. W. *Acc. Chem. Res.* **1994**, *27*, 302. (b) Fabbrizzi, L.; Poggi, A. *Chem. Soc. Rev.* **1995**, *24*, 197. (c) Tsien, R. Y. *Am. J. Physiol.* **1992**, *263*, C723. (d) James, T. D.; Linnane, D.; Shinkai, S. *Chem. Commun.* **1996**, 281. (e) *Probe Design and Chemical Sensing, Topics in Fluorescence Spectroscopy*; Lakowicz, J. R., Ed.; Plenum: New York, 1994; Vol. 4, p 109.

(8) For example: (a) Das, S.; Thomas, K. G.; Thomas, K. J.; Kamat, P. V.; Geoge, M. V. *J. Phys. Chem.* **1994**, *98*, 9291. (b) MacQueen, D. B.; Schanze, K. S. *J. Am. Chem. Soc.* **1991**, *113*, 6108. (c) Delmond, S.; Letard, J. F.; Lapouyade, R.; Matheret, R.; Jonusauskas, G.; Rulliere, C. *New J. Chem.* **1996**, *20*, 861.

(9) For example: (a) Yamauchi, A.; Takashita, T.; Nishizawa, S.; Watanabe, M.; Terame, N. *J. Am. Chem. Soc.* **1999**, *121*, 2319. (b) Marquis, D.; Desevergne, J.-P.; Bouas-Laurrent, H. *J. Org. Chem.* **1995**, *60*, 7984.

(10) McFarland, S. A.; Finney, N. S. *J. Am. Chem. Soc.* **2001**, *123*, 1260−1261.

(11) Lehn, J.-M. *Supramolecular Chemistry, Concepts and Perspectives*; VCH: Weinheim, Germany, 1995.

(12) See: *Chem. Eng. News*. **1998**, *67*, 37.

(13) (a) Ji, H.-F.; Dabestani, R.; Brown, G. M. *J. Am. Chem. Soc.* **2000**, *122*, 9306−7. (b) Ji, H. F.; Dabestani, R.; Sacheleben, R. A. *Chem. Commun.* **2000**, 833. (c) Ji, H.-F.; Brown, G. M.; Dabestani, R. *Chem. Commun.* **1999**, 609.

(14) Shen, Y.; Sullivan, B. P. *Inorg. Chem.* **1995**, *34*, 6235.

(15) Peo, S.; Godwin, H. A. *J. Am. Chem. Soc.* **2000**, *122*, 174.

(16) Beer, P. D.; Gale, P.; Smith, D. K. *Supramolecular Chemistry*; Oxford University Press: New York, 1999.

(17) (a) Xia, W.-S.; Schmehl, R. H.; Li, C.-J. *J. Am. Chem. Soc.* **2000**, *122*, 5599. (b) Xia, W.-S.; Schmehl, R. H.; Li, C.-J. *Chem. Commun.* **2000**, 695.

(18) *SHELXTL-PLUS*, version 5.1; AXS Bruker: Madison, WI, 1997.

(19) *Standards in Fluorescence Spectrometry, Ultraviolet Spectrometry Group*; Miller, J. N., Ed.; Chapman and Hall: New York, 1981.

(20) Sandros, K.; Sundahl, M.; Wennerstrom, O.; Norinder, U. *J. Am. Chem. Soc.* **1990**, *112*, 3082.

(21) Battino, F. A.; Scarllata, G.; Sciotto, D.; Torre, M. *Tetrahedron* **1982**, *38*, 3712.

(22) k_r was determined by $k_r = \Phi/\tau_r$. See: Balzani, V.; Scandola, F. *Supramolecular Photochemistry*; Ellis Horwood Limited: New York, 1991.

(23) *NMR of Macromolecules, a Practical Approach*; Gordon, C. K., Ed.; IRC Press: New York, 1993.

(24) (a) Maeda, T.; Kimura, K.; Shono, T. *Bull. Chem. Soc. Jpn.* **1982**, *55*, 3506. (b) Maeda, T.; Ouchi, M.; Kimura, K.; Shono, T. *Chem. Lett.* **1981**, 1573. (c) Ikeda, I.; Katayama, T.; Okahara, M.; Shono, T. *Tetrahedron Lett.* **1981**, *22*, 3615. (d) Handyside, T. M.; Lockhart, J. C.; Macdonnell, M. B.; Rao, R. V. S. *J. Chem. Soc., Dalton Trans.* **1982**, 2331. (e) Marson, E.; Eick, H. A. *Acta Crystallogr., Sect. B* **1982**, *1*, 1821.

(25) For example: (a) Bhagwat, V. W.; Manohar, H.; Poonia, N. S. *Inorg. Nucl. Chem. Lett.* **1981**, *17*, 207. (b) Xu, W. X.; Clinger, K.; Hackert, M. L.; Poonia, N. S. *J. Inclusion Phenom.* **1985**, *3*, 163.

(26) For example: (a) Domasevitch, K. V.; Ponomareva, V. V.; Rusanov, E. B. *J. Chem. Soc., Dalton Trans.* **1997**, 1177. (b) Vidal, J. L.; Shoening, R. C.; Troup, J. M. *Inorg. Chem.* **1981**, *20*, 227.

(27) Kleinpeter, S. S.; Holdt, H. J. *Magn. Reson. Chem.* **1991**, *29*, 999.

(28) Hill, S.; Lockhart, M. N.; Masley, L. C.; David, P. *J. Chem. Soc., Dalton Trans.* **1996**, *7* (9), 1459.

(29) Wang, D.; Sun, X.; Hu, H.; Liu, Y.; Chen. B. *Polyhedron* **1989**, *8*, 2051.

(30) Arnim, H. von; Dehnicke, K.; Maczek, K.; Fenske, D. *Z. Naturforsch.* **1993**, *48b*, 1331.

(31) Turro, N. J. *Modern Molecular Photochemistry*; Benjamin Cummings Publishing Co.: Menlo Park, CA, 1978.

(32) (a) Sharaffy, S.; Muszkat, K. A. *J. Am. Chem. Soc.* **1971**, *93*, 4119. (b) Geogiou, D.; Muszkat, K. A.; Fischer, E. *J. Am. Chem. Soc.* **1968**, *90*, 3097.

(33) (a) Tabishi, I.; Yuan, L. C. *J. Am. Chem. Soc.* **1981**, *103*, 3574. (b) Syamala, M. S.; Devanatha, S.; Ramamurthy, V. *J. Photochem.* **1982**, *34*, 219.

(34) Duveneck, L. G.; Sitznann, K. B.; Turro, N. J. *J. Phys. Chem.* **1989**, *93*, 7166.

(35) Sandanyke, K. R. A.; Nakashima, K.; Shinkai, S. *Chem. Commun.* **1994**, 1621.